JOURNAL OF SOLID STATE CHEMISTRY 54, 34–48 (1984)

The Acceleratory Degradation of Solids According to Non-Steady-State Kinetics

JOSEPH D. DANFORTH, SCOTT R. PORTER, AND DAVID STRICKLER

Grinnell College, Grinnell, Iowa 50112

Received October 25, 1983; in revised form February 13, 1984

The acceleratory degradation of solids represents an area of research where extreme care must be exercised to obtain reproducible data. Different preparations of the same substance often show great variation in degradation patterns. Many kinetic equations have been developed to describe the kinetics of acceleratory degradations. Most of them are empirical and apply only to certain phases of a degradation. The non-steady-state kinetics which were developed to describe the zip degradation of poly(vinyl chloride) will be shown to describe effectively the unusual degradation behavior of inorganic solids that follow an acceleratory pattern.

Introduction

Young (*1*) has described the isothermal kinetics for the acceleratory reaction, $A_{(s)} \rightarrow B_{(s)} + C_{(g)}$. He recognized five features of acceleratory reactions: there may be an initial evolution of trace amounts of gas, there may be an induction period, there will be an acceleratory phase and a deceleratory phase, and for some degradations there may remain significant amounts of residual solid that does not decompose. Plots of α, the fraction decomposed, as a function of time give sigmoidal curves that are characteristic of acceleratory degradations. Plots of rate as a function of time or α show an acceleratory phase, a maximum rate, and a deceleratory phase.

An additional characteristic of acceleratory degradations is their lack of reproducibility. Aged samples behave differently from fresh samples and each preparation appears to have an induction period and a kinetic behavior that differs from another preparation.

One of the challenges of solid state chemistry has been to describe the kinetics and mechanisms that are responsible for acceleratory behavior. Reviews of theories which have been developed to explain acceleratory behavior have been given by Jacobs and Tompkins (*2*) and Young (*1*). Fox and Hutchinson (*3*) have reviewed degradation schemes that apply to azides. In spite of extensive work there is no single theory which satisfactorily predicts all phases of acceleratory behavior. However, Ng has suggested a single empirical equation that adequately represents some of the equations that have been used to characterize various phases of acceleratory degradations (*4*). It is customary that one of these theoretical or empirical equations is used during the acceleratory phase and then a completely different equation will be used for the deceleratory phase. Thus, Haines and Young found that silver oxalate accelerated according to an exponential law and decayed according to a contracting sphere model (*5*). Some investigators have consid-

0022-4596/84 $3.00

ered as many as four equations to characterize a single degradation reaction (*6*). The theoretical models (*3*) which seem best for the acceleratory phase are based on the concepts that germ nuclei on the surface become growth nuclei by an initiation process. The growth nuclei expand along the surface during acceleration. When growth nuclei begin to overlap, deceleration begins. The deceleration has been described in terms of a contracting volume expression (*7*), the Erofeev equation (*8*), and the Avrami equation (*9*).

Poly(vinyl chloride) decomposes by acceleratory kinetics giving degradation patterns of evolved hydrogen chloride that are practically superimposable upon evolved gases from lead azide, lithium azide, silver oxalate, and potassium *tris* (oxalato) ferrate. The non-steady-state kinetics (NSSK) which effectively characterize PVC degradations (*10–12*) will be shown to apply to the acceleratory degradations of these inorganic compounds.

NSSK are based on the zipper mechanism. Chain initiation occurs at discrete positions along a PVC chain. Once a chain has been initiated, it unzips producing hydrogen chloride. The initiation reaction accounts for insignificant production or consumption of hydrogen chloride. The zip reaction is responsible for practically all of the hydrogen chloride evolved. The initiation reaction even though it involves only negligible amounts degradation has a very significant influence on the degradation pattern. Trace impurities can prevent chain initiation and are often responsible for long induction periods. The number of initiation sites that form zip chains influences the average length of a zip chain and the length of the zip chain, in turn, influences the time at which the maximum degradation rate is observed. Thus, minor changes in initiation behavior result in major changes in degradation patterns. Initiated zip chains require relatively long times to unzip. Acceleration occurs during the buildup of zip chains. Deceleration occurs when more chains are terminating than are starting.

An analogous process will be suggested for inorganic solids. Initiation occurs at the surface and degradation proceeds by a chain reaction growing in one dimension which is separate and distinct from the initiation reaction. A reaction chain operates primarily within its own domain whether that domain is a PVC molecule or a discrete globule of a crystalline or amorphous inorganic solid. The length of the reaction chain will depend upon the number of initiations in each domain, and the size of the domain. Reaction chains build up during the acceleratory phase and are removed from production as they go to completion during the deceleratory phase. The unusual features of acceleratory degradations will be effectively accounted for by NSSK.

Experimental

An apparatus which gives an accurate measurement of α and $\Delta\alpha$/interval as a function of time has been described (*10–14*). Samples in quartz crucibles are introduced to a reaction chamber that is maintained at a constant temperature. Evolved gas is measured at uniform intervals. From these measurements and the loss in weight of the sample, α and $\Delta\alpha$/interval are calculated for each time. Data are stored in a computer. The best values of parameters for several non-steady-state kinetic equations can be determined by appropriate computer programs (*15*).

A different computer program generates simulated degradations for single samples and for mixtures containing as many as 10 samples for assigned values of parameters. Simulated runs for single samples were, of course, fitted exactly by the appropriate non-steady-state equation and mixed samples gave satisfactory agreement of calculated and observed data at approximately

the weighted averages of the assigned parameters (*15*).

Runs have been made using three different schemes: (1) The sample was initiated and degraded at a single temperature. (2) The sample was initiated to reach an arbitrary value of α, the fraction degraded, at one set of conditions, removed from the chamber and allowed to stand exposed to the atmosphere and then reintroduced to the chamber at the same temperature or at some lower temperature. (3) The sample was initiated at a high temperature, cooled rapidly within the chamber in flowing helium to a lower temperature and then degraded at the lower temperature.

The sample preparations, run numbers, run conditions, and pertinent observations are summarized for substances studied in this report.

Poly(vinyl chloride), Run 1. A sample from Scientific Polymer Products (100.9 mg, degree of polymerization 1381) was degraded for 8 min at 230°C until acceleration was occurring. The chamber was quickly cooled to 200°C and the rate allowed to line-out during the next 11 min. At this point the sample had lost only 3.0% of its hydrogen chloride. The run was continued for 3.5 hr. No perceptible degradation occurred when

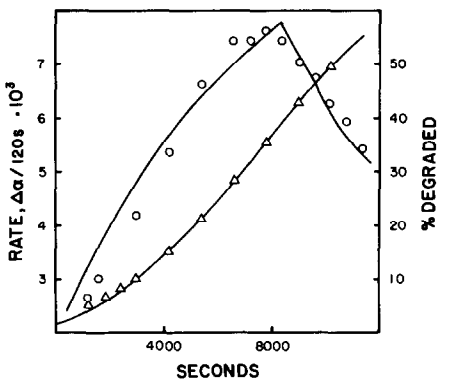

FIG. 1. Rate and percentage degraded as a function of time for prestarted PVC at 200°C. (○) Rate, (△) percentage degraded. Lines are calculated from best-fit parameters.

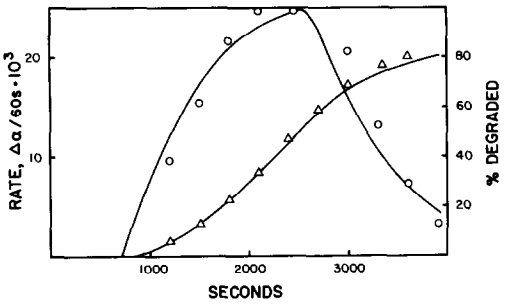

FIG. 2. Rate and percentage degraded as a function of time for lithium azide at 190°C. (○) Rate, (△) percentage degraded. Lines are calculated from best-fit parameters.

the sample was introduced originally at 200°C. Figure 1 shows plots of α and $\Delta\alpha/120$ sec vs time. The symbols represent data and the lines represent calculated values of α and $\Delta\alpha/120$ sec.

Lithium Azide

A sample from Eastman Organic Chemicals was dissolved in water, filtered, evaporated on a rotary evaporator then precipitated by the addition of ethanol. Mushy crystals representing only a small fraction of the original solid were filtered and dried by standing in a desiccator over P_2O_5 in the dark.

Run 2. An amount of 27.2 mg was degraded at 190°C. The sample lost 19.9 mg (23.3 mg theory). Figure 2 shows data (symbols) and calculated values (lines) for α and $\Delta\alpha/60$ sec as a function of time. It was not established whether incomplete degradation was caused by the presence of inert impurities or by the formation of lithium nitride. The important observation is that the evolved nitrogen followed NSSK.

Lead Azide

Fifty milliliters 0.2 *M* potassium azide was added dropwise with stirring to 30 ml 0.1 *M* lead nitrate. The precipitate was dried for 3 hr at 110°C and stored in the dark.

Run 3. An amount of 100.5 mg was introduced at 250°C and the temperature raised to 260°C where acceleration began. At 260°C relative peak areas in order of appearance at 60-sec intervals were 2, 6, 12, 26, 48, 70, 96, 120, 146, 168, 196, 216, 252, 288—explosion. The quartz crucible was completely shattered.

Run 4. An amount 49.0 mg of the same sample on the same day was degraded at 250°C. After a 19-min induction period during which negligible peaks of nitrogen were observed, the recording of peaks was begun. The sample was assumed to have degraded completely. A plot of $\Delta\alpha/60$ sec vs t (symbols) is compared with $\Delta\alpha/60$ sec calculated from the parameters at best fit (the line) in Fig. 3 (upper curve).

Run 5. After standing in the dark for 3 months, 92.8 mg of lead azide was subjected during a single run to the following temperatures with the following observations: 245°C—only traces of gas during 45 min, raise to 250°C—only traces of gas during an additional 51 min. At 260°C only traces of gas for 20 min at which time the acceleratory reaction began. The reaction temperature was reduced to 245°C and a normal acceleratory degradation was observed. The degradation was interrupted for measurements that are not pertinent to this paper. The run is reported to illustrate the dramatic effects of aging. The fresh sample had an induction period of 19 min at 250°C. The aged sample had an induction period of 106 min at 245–260°C. During the induction period trace amounts of nitrogen were formed.

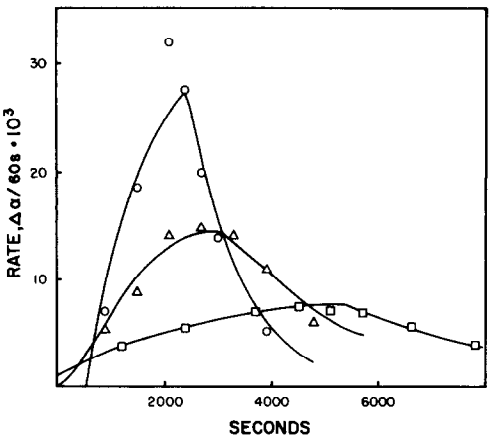

FIG. 3. Rates of lead azide degradations. (○) Fresh sample at 250°C, (△) aged sample at 245°C, (□) aged sample at 235°C. Lines are calculated from best-fit parameters.

Run 6. Aged lead azide (93.0 mg) was introduced at 250°C, and the temperature raised to 260°C where acceleration began. At the start of acceleration, peaks were recorded and the temperature lowered quickly to 245°C where a normal acceleratory run was made. The run was discontinued after 83 min. The weight loss was 21.7 mg. Rate as a function of time is shown in Fig. 3 (middle curve). When the run was discontinued, peak heights extended above the midpoint of the chart paper. The sample was allowed to stand in the crucible exposed to air for 2.5 hr. and then returned to the reaction chamber at 245°C. Only trace nitrogen peaks could be detected.

Run 7. Aged lead azide (97.9 mg) was initiated at 260–265°C during 13–15 min and cooled quickly to 235°C where the run was continued for 3 hr. The sample lost 23.4 mg. Rate data as a function of time are shown in Fig. 3 (lower curve).

Silver Oxalate

Silver oxalate precipitated from stoichiometric quantities of silver nitrate and oxalic acid was dissolved in concentrated ammonia, filtered, and reprecipitated by the dropwise addition of 70% perchloric acid. After drying under vacuum at 50°C the powder was stored in the dark. The sample was separated into large and small crystals by shaking on a 100-mesh sieve. Only a negligible proportion of small crystals passed through the sieve. The large crystals gave essentially the same degradation pattern as the original sample. Runs 8

and 9 were made two weeks after the crystals were prepared.

Run 8. Large crystals (53.0 mg) were degraded at 130°C to lose 14.1 mg (15.4 mg theory). A rate–time plot is shown in Fig. 4.

Run 9. Small crystals (49.7 mg) were degraded at 130°C to lose 13.6 mg (14.4 mg theory). A rate–time plot is shown in Fig. 4.

Run 10. Silver oxalate (102.0 mg) which had aged for 17 months was initiated by heating to 145°C. When acceleration began, the sample was cooled rapidly in the chamber under helium to 115°C where it was degraded for an additional 143 min. The sample had lost 9.3% of theory during prestart and lining out at the run temperature. The sample was removed when the weight loss was 61.2% of theory and the relative peak areas were 25 units. After standing in the atmosphere for 10 min the sample was returned to the chamber. Relative peak areas were initially 8, and attained 16 after 18 min. When the sample was removed and allowed to stand for 16 hr. peak areas were negligible at the beginning but soon began the acceleratory behavior. A plot of rate ($\times 10$) as a function of time for the initial degradation is shown in Fig. 4.

Run 11. Clear green crystals of $K_3Fe(C_2O_4)_3 \cdot 3H_2O$ (102.7 mg) were charged to a quartz crucible and dehydrated at 200°C in the reaction chamber under intermittent flow of helium until the sweep-out with helium produced no discernible water peak. The crucible was removed from the chamber and weighed. The loss in weight was 11.1% due to evolution of water (theory 11.0%). The temperature of the reaction chamber was raised to 250°C and the crucible reintroduced. After 18 min during which CO_2 peaks were extremely small or zero the run was started. Peaks were recorded every 60 sec for a period of 7740 sec when the run was discontinued. Carbon dioxide peaks of significant area were still being produced. The loss in weight of CO_2 was 8.0 mg. Complete loss of CO_2 would correspond to 9.0 mg.

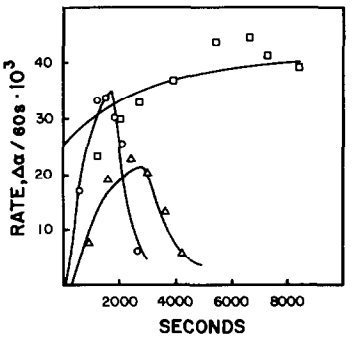

FIG. 4. Rates of silver oxalate degradations. (○) Small particles at 130°C, (△) large particles at 130°C, (□) aged particles at 115°C, latter rate multiplied by 10. Lines are calculated from best-fit parameters.

Computer Storage and Analysis of Data

The fraction degraded, α, and the rate, $\Delta\alpha$/interval, from best-fit parameters and from actual data are calculated and stored for each interval. Simulated runs for single and mixed samples were prepared by entering calculated rates for the various parameter assignments as observed peak areas are entered for an actual run.

The best-fit program has many options. In prior work an equation was used that was based on certain reasonable but complicated assumptions about the way chain termination occurred in PVC (*11*). Error was expressed as percentage difference per fitted point. In the present work it has been assumed that chain termination occurs evenly throughout a run. To account for incomplete degradation, if it should occur, the ideal equation (no chain termination) is merely multiplied by a constant, α_∞, to allow α values less than 1.0 at long times. When degradation is complete as it has been assumed to be for most of the inorganic samples, the different equations are identical and are represented by the ideal equation which will subsequently be described. In this work the best fits unless otherwise specified have been based on mini-

mizing the percentage error per fit point. Since small peaks may have substantial integrator error on a percent error per peak basis, best fits were obtained over the degradation range, 0.05 to (final α − 0.05).

The fundamental assumption underlying the kinetic model is that the degradation rate will equal the fraction of reaction chains that is degrading times the fraction of a chain degrading per second. The term, equal, is appropriate because, when data are expressed in terms of fractions, the proportionality constants normally used in such expressions cancel out. It is further assumed that started reaction chains continue to produce volatile product until they are completely degraded. When a reaction chain goes to completion, it is removed from production. The ideal differential equation which applies to samples that degrade completely (α_∞ = 1.0) has been shown to be (*10*). From $t = 0$ to $t = 1/k_z$

$$d\alpha/dt = k_z(1 - e^{-k_i t}) \quad (1)$$

From $t = 1/k_z$ to $t = \infty$

$$d\alpha/dt = k_z(1 - e^{-k_i t}) - k_z(1 - e^{-k_i(t-1/k_z)}). \quad (2)$$

There is no discontinuity at $t = 1/k_z$. The constant, k_i, is the fraction of total reaction chains initiating per second, and k_z is the fraction of a started chain that reacts per second. The integrated forms (*10*) of these equations were used to obtain calculated values of the fraction decomposed that had the smallest percentage error per fitted point.

In addition to the parameters, k_i and k_z, the best-fit program allows a time shift, t_s, which in effect moves the calculated data to the right or left along the time axis but does not alter the shape of the degradation curve. As expected prestarted samples have negative time shifts and samples having induction periods have positive time shifts. Runs were started when observed peak areas became significant so recorded time shifts do not normally include the long induction periods.

Results and Discussion

Based upon our extensive work on acceleratory degradations of inorganic and organic substances, it appears that a non-steady-state kinetic model developed on the basis of the zipper mechanism for PVC, effectively represents acceleratory degradations. That model is based upon first-order initiation of reaction chains which then degrade at a constant rate. Alternative orders of initiation and chain degradation have been evaluated and will be described in a later publication. All of the non-steady-state models give representations of data over the entire range of a degradation that seem superior to other kinetic models. None of these alternate non-steady-state models, however, was significantly better in representing data than the model used in this paper. That model is based on first-order initiation and zero-order chain degradation.

In order to establish the general application of NSSK to acceleratory degradations of PVC and representative inorganic substances, specific examples will be presented to illustrate degradation patterns. Preheating techniques will be described which make it practical to obtain degradation data at temperatures where the induction period would be excessive. Different poisoning behaviors on the exposure of degrading chains to the atmosphere will be described, and other equations normally used for solid state degradation will be shown to apply correctly over limited ranges of our data.

Preinitiation Behavior and the Degradation Patterns of PVC

Degradation curves for PVC samples of varying chain lengths have been described (*11, 12*). These curves appear to be practi-

cally superimposable upon the degradation curves for inorganic substances. Degrading samples of PVC, removed from the chamber and exposed to the atmosphere for long times, will immediately resume their earlier degradation rates when returned to the reaction chamber (*11*). Samples which have been partially degraded at an elevated temperature will exhibit significant acceleratory degradation at temperatures far below the temperature at which degradation can be initiated in the original sample (*10*). Preinitiation techniques for PVC have also been used in our work on inorganic substances. A preinitiation for PVC is illustrated in Fig. 1 for a sample that was initiated at 230°C, cooled rapidly to 200°C and degraded at this temperature for 3.5 hr. Values of percentage of degradation and $\Delta\alpha/120$ sec for the data (symbols) and calculated from best-fit parameters (lines) are shown. Best-fit parameters were $k_i = 1.35 \times 10^{-4}$ sec^{-1}; $k_z = 1.01 \times 10^{-4}$ sec^{-1}; $\alpha_\infty = 0.87$; $t_s = -1557$ s; $\Delta = 0.41\%$ difference per fitted point. Preinitiation at 230°C is essential. Without preinitiation only negligible degradation occurred for many hours at 200°C.

Plots of percentage of degradation and $\Delta\alpha/120$ sec as a function of time show good agreement of theory and data. Differences, which are emphasized in the rate plot, may be at least in part due to the use of single-valued parameters in a situation where a mixture of parameter values probably exists. The time shift of -1557 sec is interpreted as the time at which the acceleratory degradation would have started if the entire run had been made at 200°C. The initiation of the acceleratory reaction at 200°C would undoubtedly have been preceded by a very long induction period. An α_∞ value of 0.87 is reasonable and proper based on our previous knowledge of PVC degradations.

The data for PVC degradations seem to be represented effectively by the NSSK model based on a zipper mechanism.

Degradation Characteristics of Lithium Azide

Figure 2 shows rate and percent degraded vs time for lithium azide. The symbols represent the data and the lines represent calculated data for the range of 0.05 to 0.80 α. The $\alpha - t$ plots as expected show good agreements of data (symbols) and calculated values (lines). Good agreement is also shown for the more critical evaluation in which rate is plotted as a function of time. Best-fit parameters were

$$k_i = 1.33 \times 10^{-3} \text{ sec}^{-1};$$

$$k_z = 5.39 \times 10^{-4} \text{ sec}^{-1},$$

$$\alpha_\infty = 0.85,\ t_s = 720 \text{ sec};\ \Delta = 4.1$$

(% error per point). The value of 0.85 for α_∞ was chosen and fixed to agree with the observation that the loss in weight was only 85% of theory even though the degradation was complete. The maximum rate calculated and the maximum rate observed appear at approximately the same time and a time shift of +720 sec is appropriate since the acceleratory portion of the reaction was preceded by an induction period during which very small peaks were observed. This lithium azide sample was allowed to degrade completely. Other samples when removed at a time when they were producing large nitrogen peaks gave only trace nitrogen peaks when returned to the chamber after 1 hr exposure to the atmosphere. The degradation of lithium azide has been shown to be catalyzed by the presence of lithium metal and to be inhibited by water or air (*16*). In our degradation scheme the chain reaction is represented by the formation of lithium metal within its own domain. Exposure to the atmosphere presumably destroys the lithium at the end of the propagating chain and stops the degradation. Induction periods normally encountered in the degradation of lithium azide represent a period during which impurities in the sam-

ple destroy the lithium metal as fast as it forms. Acceleratory degradation begins only after the active impurities have been destroyed by reaction with lithium.

Degradation Characteristics of Lead Azide

Best fits and data for fresh and aged lead azide and for an aged sample that was initiated at 260°C and degraded at 235°C are compared in Fig. 3. Parameters at best fit are summarized in Table I. The fresh sample at 250°C started acceleratory degradation after an induction period of only 19 min. The same sample after aging did not start acceleratory degradation after 45 min at 245°C and an additional 51 min at 250°C. When the temperature was raised to 260°C the acceleratory degradation finally began. The fresh sample exploded at 260°C but showed normal acceleratory behavior at 250°C.

The agreement between the data (symbol) and values calculated from best-fit parameters (lines) indicates that the kinetic model is appropriate for lead azide under a variety of degradation conditions. The model represents both aged and fresh samples. Calculated maximum rates appear at times that do not differ significantly from observed maxima. The two samples which were preinitiated show negative time shifts as expected. The sample initiated and run at 250°C shows a positive time shift which is necessary to account for slow degradation during an induction period. An aged sample which was producing copious quantities of nitrogen ceased degradation entirely after exposure to the atmosphere at room temperature for 2.5 hr.

Hutchinson *et al.* (*17*) fit decomposition data for a single sample of lead azide by a single equation developed from concepts of the shrinking sphere model. The shrinking sphere model implies that $\alpha^{1/3}$ is proportional to t. It is not unusual that a single sample of lead azide follows this model but as will be subsequently shown, it would be most unusual if all samples of lead azide followed that model.

The kinetic equations based on nonsteady-state zip kinetics effectively represent the exotic behaviors of lead azide under a variety of conditions. The initiation site, as recognized by others is an atom of lead. In our model, the atom of lead in the degrading chain "eats its way" through a domain. The fewer the initiation sites and the larger the domain, the longer will be the reaction chains and the smaller will be k_z, the fraction of a chain degrading per second. Only a single atom of lead, the one most recently deposited, acts as a site for continuing the reaction chain. Concepts of chain branching in which one atom starts two chains or whereby every lead atom produced acts as a permanent degradation site predict rates of acceleration greatly in excess of those actually observed. The complete loss of activity on exposure to the atmosphere can be explained on the basis of the destruction of the active site by reaction with water vapor (*18*). Probably oxygen would also destroy the active site.

TABLE I

BEST-FIT PARAMETERS FOR LEAD AZIDE

Run	$k_i \times 10^3$ (sec^{-1})	$k_z \times 10^3$ (sec^{-1})	α_∞[a]	t_s (sec)	Δ (% error/pt.)
6	0.80	0.28	1.0	242	4.6
7	0.27	0.17	1.0	−545	0.6
4	1.0	0.48	1.0	523	6.4

[a] Arbitrarily held at 1.0 corresponding to the assumption that degradation would be complete. When degradation is complete the ideal NSSK equation applies.

Degradation Characteristics of Silver Oxalate

The agreement of theory and data for the decomposition of large and small crystals of silver oxalate is shown in Fig. 4. Values of

TABLE II

BEST-FIT PARAMETERS FOR SILVER OXALATE, LARGE AND SMALL PARTICLES

Run	$k_i \times 10^3$ (sec^{-1})	$k_z \times 10^3$ (sec^{-1})	α_∞[a]	t_s (sec)	Δ (% error/pt.)
8	0.83	0.40	1.0	326	4.2
9	1.6	0.62	1.0	166	1.99

[a] Arbitrarily held at 1.0 corresponding to the assumption that degradation would be complete.

the parameters are summarized in Table II. The large crystals are essentially the same as the entire sample because the small crystals passing through the 100-mesh sieve represented only a very small proportion of the sample. As would be expected the large crystals had a longer chain length characterized by a smaller value of k_z and required a longer time to reach their maximum degradation rate. A run initiated at 145°C and run at 115°C shows the characteristic broad maximum and the negative time shift observed for all species initiated at a high temperature and subsequently run at a lower temperature. The negative time shift of −3044 sec gives an estimate of the time the run would have started if the initiation and run had been at 115°C. Parameter values were $k_i = 0.00032\ sec^{-1}$, $k_z = 0.00069\ sec^{-1}$, $\alpha_\infty = 1.0$, $t_s = -3044$ sec, $\Delta = 4.3\%$ error per point.

Exposure to the atmosphere of a sample that was producing copious amounts of CO_2 reduced and eventually stopped the evolution of CO_2. The sensitivity to exposure, though definitely existing, is not nearly as critical for silver oxalate as it is for the azides.

Haynes and Young (*5*) recognized the irreproducible behavior of freshly prepared silver oxalate and stabilized that behavior by annealing. They found that the Prout–Tompkins equation (*19*) fit the acceleratory data and that the contracting sphere equation fit the decay period. Leiga (*20*) found that silver oxalate degradations could be represented by the equation $\alpha = Ct^n$ where values of n varied from 3 to 5.

The non-steady-state kinetics which are proposed in this paper give good fits of data for aged samples, fresh samples, and both large and small particles. Furthermore, these fits are obtained over the entire range of a degradation.

Degradation Characteristics of Potassium tris(oxalato) Ferrate

The degradation behavior of potassium *tris*(oxalato) ferrate initiated and run at 250°C is illustrated in Fig. 5. The evolved gas is CO_2. Rates and α are plotted as a function of time. The agreement of data (symbols) and calculated values (line) illustrates that the non-steady-state model applies. On exposure to the atmosphere after partial degradation the behavior of this inorganic substance resembles the behavior of PVC. The sample rapidly resumes its previous rate of degradation after exposure. The chain propagating substance in this instance is apparently not destroyed on exposure to the atmosphere. The values of the parameters that give the best reproduction of the data were $k_i = 0.000375\ sec^{-1}$, $k_z = 0.00021\ sec^{-1}$, $\alpha_\infty = 1.00$, $t_s = 132$ sec, $\Delta = 2.32\%$.

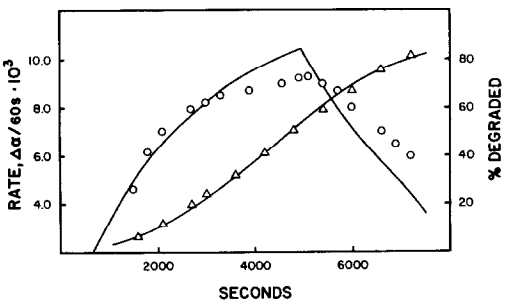

FIG. 5. Rate and percentage degraded as a function of time for potassium *tris*(oxalato) ferrate at 250°C, (○) rate, (△) percentage degraded. Lines are calculated from best-fit parameters.

The Application of Conventional Solid State Equations to Data and Calculated Best-Fit Values

The Avrami–Erofeev, the power-of-t, and the contracting-volume equations have been used to correlate acceleratory degradations. The Avrami–Erofeev and the power-of-t equations can be applied to the acceleratory phase of a degradation while the contracting-volume equation applies only to the deceleratory phase.

In order to illustrate that the data used in our correlations conform to conventional equations that have been suggested by others, selected data have been correlated using these other equations. Calculated data for best-fit values of parameters have also been correlated to illustrate that the non-steady-state model based on zipper kinetics gives degradation behaviors that are expected on the basis of equations that have been used by others to correlate such data.

The Power-of-t Equation

Figure 6 shows plots of $\alpha^{1/n}$ (n = 2, 3, and 4) vs t for degradations of lead azide at 235, 250, and 260°C. For the prestarted sample (Run 7, Curve A) at 235°C there is excellent agreement of both data and theory with the square of the time ($\alpha^{1/2}$ vs t gives a straight line). At 250°C data and calculated points show agreement with t^3 ($\alpha^{1/3}$ vs t gives a straight line, Curve B). For Run 3 at 260°C

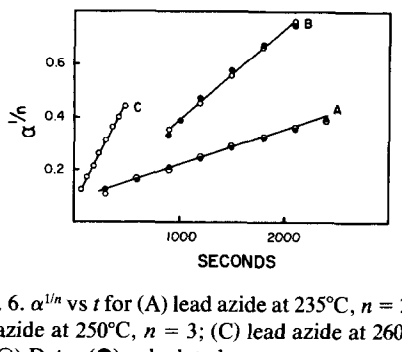

FIG. 6. $\alpha^{1/n}$ vs t for (A) lead azide at 235°C, n = 2; (B) Lead azide at 250°C, n = 3; (C) lead azide at 260°C, n = 4. (○) Data, (●) calculated.

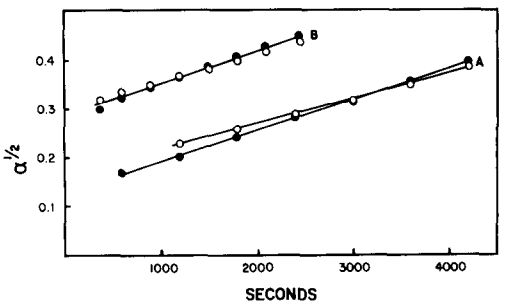

FIG. 7. $\alpha^{1/2}$ vs t for (A) PVC at 200°C; (B) silver oxalate at 115°C. (○) Data, (●) calculated.

the cumulative volume which is proportional to α shows a t^4 relationship (cum. Vol.$^{1/4}$ vs t gives a straight line, Curve C).

It seems significant that the same material under different conditions obeys the power-of-t equation for exponents 2, 3, and 4 and that NSSK predict that this behavior is expected for appropriate values of k_i and k_z. Values of k_i and k_z that give rapid acceleration can give exponent values of time greater than 2. On the basis of our NSSK model there is no special significance when an occasional behavior corresponds to an integer exponent greater than 2. The t^2 relationship appears to be theoretically significant and is characteristic of samples that have been initiated at a high temperature and then degraded at a lower temperature.

As shown in Fig. 7 silver oxalate and PVC exhibit the same t^2 relationship that was shown for lead azide in Fig. 6.

The rates, of course, show the constant accelerations necessary for α to be proportional to t^2. The t^2 relationship for α and the t relationship for rate can be expected for small values of $k_i t$ that occur when samples are degraded at low temperatures. Thus, Eq. (1) becomes $d\alpha/dt = k_z k_i t$ when the e^x expansion, neglecting higher powers, is used for $e^{-k_i t}$.

The Avrami–Erofeev Equation

The Avrami–Erofeev equation with n = 3

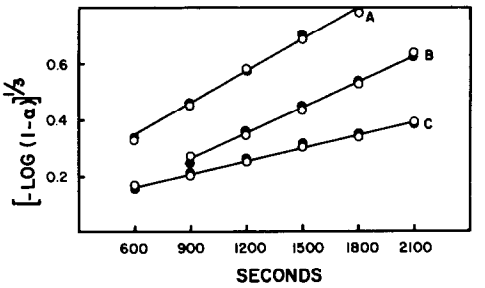

FIG. 8. Avrami–Erofeev plots. (A) Silver oxalate at 130°C; (B) lead azide at 250°C, potassium *tris*(oxalato) ferrate at 250°C; (○) data, (●) calculated.

has been used to correlate data for the degradation of lithium azide (*16*). Plots of $[-\log(1-\alpha)]^{1/3}$ vs t gave straight lines during the acceleratory phase. Figure 8 shows similar Avrami–Erofeev plots for silver oxalate, 130°C (Curve A), lead azide, at 250°C (Curve B), and potassium *tris*(oxalato)ferrate at 250°C (Curve C). Both calculated and data points follow the Avrami–Erofeev relationship during the acceleratory phase.

The Contracting-Volume Equation

The contracting volume equation $1-(1-\alpha)^{1/3} = k_2t$, has been used to correlate acceleratory degradations during the deceleratory phase (*16*). Figure 9 shows the correlation of calculated points for silver oxalate at 130°C (Curve A), lead azide at 250°C (Curve B), and potassium *tris*(oxalato) ferrate at 250°C (Curve C).

It is not surprising that data during the deceleratory phase are effectively represented by the contracting-volume equation since similar correlations have often been reported. It does seem significant that the NSSK model with appropriate choice of parameters predicts contracting-volume kinetics during the deceleratory phase.

Discussion of the Non-steady-State Model

The non-steady-state model based on a zip mechanism effectively represents both acceleratory and deceleratory phases for PVC and a variety of inorganic compounds. Appropriate assignment of the parameters k_i, the fraction of chains initiating per second, and k_z, the fraction of a chain degrading per second gives calculated values that conform to (a) the power-of-t equation with exponents of 2, 3, and 4; (b) the Avrami–Erofeev equation, and (c) the contracting-volume equation. Conformity with powers of t greater than two seems to be a coincidence. Conformity to a power of t equal to 2 is expected on the basis of the rate assumptions underlying the non-steady-state model.

Because of the apparent general applicability of the kinetic model, it seems appropriate to discuss some of its features and to point out the ways in which it agrees with and differs from previously proposed kinetic schemes.

MacDonald (*21*) considered hypothetical models for the degradation of silver oxalate. In one of these models he assumed that nuclei present initially and nuclei forming spontaneously grew as chains in one dimension only. The number of nuclei on each crystallite was "not very great." As long as the chains from the nuclei present originally continued to produce, he suggested that the rate would be given by the expression

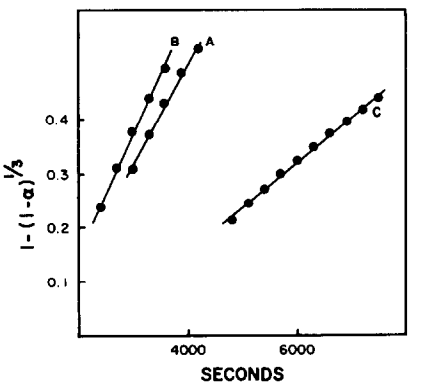

FIG. 9. Contracting-volume plots. (A) Silver oxalate at 130°C; (B) lead azide at 250°C; (C) potassium *tris*(oxalato) ferrate at 250°C. Calculated points only.

$$dx/dt = K_n + K't.$$

In this expression he assumed that fresh nuclei increased regularly with time.

The kinetic model based on the zipper mechanism assumes that only negligible initiated sites are present at $t = 0$ and that the formation of sites is first-order in remaining germ nuclei (places where initiation can occur). When sites are initiated, they start a chain degradation that is, for all practical purposes, confined to the crystallite or domain in which the initiation occurred. An initiated chain reacts in one dimension at a certain average fraction of a chain per second until the chain is terminated by consuming all the material in its domain. More than one initiation per domain may occur. The initiation sites and the gas evolved during initiation represent only negligible proportions of the degrading solid.

The gas formed by the chain reaction represents substantially all of the gas evolved. MacDonald assumed that chains increased in concentration with time. The new kinetics assumes that chains increase as first-order in unstarted initiation sites until some chains completely decompose, at which time they are removed from production. The assumption that chains form from unstarted chains according to first-order initiation originated from considerations of the mechanism for PVC. It seemed reasonable that one, two, or three starting positions along a PVC molecule could initiate a zip chain. The average length of that zip chain would depend upon the degree of polymerization and the number of initiation sites per molecule. Although the fraction of chains initiating per second depended upon the remaining uninitiated sites (or the number of uninitiated molecules if there is one initiation site per molecule) the fraction of a chain unzipping per second does not include a concentration term relating to the extent of the degradation reaction. During the early stages of the reaction the fraction of chains producing will be $(1 - e^{-k_i t})$ and the value of this expression will increase from zero at $t = 0$ to 1 at $t = \infty$ where all chains would be producing if chains were infinitely long. The increase with time will not be proportional to time as was assumed by MacDonald but will be logarithmic with time. The fractional increase in producing chains will decrease with time. When chains completely degrade, they are removed from production and the fraction of producing chains decreases when more chains are removed from production than are starting. The kinetic model assumes that the fraction of producing chains at any time multiplied by the fraction of a chain degrading per second, k_z, will give the rate, $d\alpha/dt$, where α is the fraction of the sample decomposed. When k_z is defined as the fraction of a chain per second, it is, of course, independent of the number of chains that have started.

The underlying assumptions closely resemble those that were suggested by MacDonald except that chains are build-up by first-order in initiating sites and chains that have completely degraded are removed from production. Acceleration is caused by the increase in the number of producing chains growing in one dimension only. Deceleration occurs when more chains terminate than are starting. When k_z is defined as the fraction of a chain degrading per second, the maximum rate will occur when the first started chains go to completion at $t = 1/k_z$.

The time of the maximum rate depends only on the value of k_z. The value of α at the maximum rate depends on the values of k_i and k_z, $\alpha_{max} = 1 + k_z/k_i(e^{-k_i/k_z} - 1)$. Since the intrinsic zip rate expressed as moles of gas · moles chain $^{-1}$ · sec^{-1} is constant, the acceleratory and deceleratory behavior must arise from changes in the number of chains that are unzipping. Until the maximum rate is achieved the function $(1 - e^{-k_i t})$ increases at an ever decreasing rate.

Beyond $t = 1/k_z$ the function removes initially started chains and the rate decreases rapidly at first and then approaches a zero-rate asymptotically. The extent of curvature beyond the maximum depends upon the value of k_i. When k_i is large the initial rise is steep and the drop off at the maximum is correspondingly steep. When k_i is relatively small, the maximum is approached more slowly, a broader maximum is observed and the drop in rate is correspondingly less severe. The rate–time curves in Figs. 1–5 generally show the sharp drop in rate after the maximum rate. A much broader cusp and slower drop in rate is shown in Fig. 3 for lead azide at 235°C.

The proposed kinetic scheme has thus been shown to conform with observed acceleratory and deceleratory behavior and to account rationally for the appearance of the maximum rates at different values of α. It also accounts for the other characteristics of acceleratory reactions which were described in the opening paragraphs of this paper. The "burst of gas" at the start of some, but not all, degradations would be expected for a substance in which a trace of a volatile substance acted as a poison for the initiated chain. Lithium azide represents such a material and water is the volatile poison. In the process of drying a sample of lithium azide powder, small particles can be effectively dried while some of the larger particles may still contain a trace of water. When this sample is introduced to the reaction chamber, the few dried particles would immediately start producing nitrogen, resulting in a "burst of gas." As the trace of water vaporizes, these initiated chains would be quenched and chains would not start again until all of the water had been removed by reaction with the lithium formed by the slow thermal degradation of lithium azide.

Induction periods, which vary tremendously with aging and sample preparation, are primarily caused by trace impurities both volatile and nonvolatile that are capable of reacting with chain initiates. Until the impurities are removed by reaction with the active component of a chain end, no sustained chain reaction can occur. The technique of preinitiation described in this paper represents a useful way to avoid long induction periods that would normally be encountered at very low temperatures where the initial degradation leading to removal of impurities is very slow. During the induction period the slow thermal degradation of the substance occurs and trace product peaks are observed. Only after chain-terminating impurities have been removed by reacting with the thermal degradation product can the acceleratory degradation begin. On the basis of this model the preheating at higher temperatures to remove the chain-stopping impurities then running at lower temperatures seems appropriate. Such a procedure makes it possible to follow degradation patterns at temperatures where induction periods would be extremely long.

The average length of a degradation chain which establishes the time of the maximum rate is very much dependent upon the number of chains started per domain. The greater the number of chains for a given domain, the larger will be k_z and the shorter the time to attain the maximum rate. Although the volatile product involved in the initiation or termination of chains is negligible, the number of degradation chains formed per domain greatly influences the degradation pattern. The number of chains attaining a sustained reaction will be extremely sensitive to impurities and relatively minor changes in run conditions. These considerations account for the difficulties of obtaining reproducible data for acceleratory reactions. It is somewhat ironic that so many investigators have been especially concerned with initial degradation rates. According to NSSK, reproduc-

ibility during the early stages of a degradation would not be expected since these initial stages would represent a period that would be greatly influenced by trace amounts of impurities. Only after trace impurities have been removed can the characteristic degradation behavior be observed. Since the NSSK model effectively represents degradation behaviors over the entire range of a degradation for both PVC and a variety of inorganic substances, it seems appropriate to summarize qualitatively the processes that occur during various stages of a degradation and to comment briefly concerning the apparent complexity of the non-steady-state equations.

When a substance that decomposes by acceleratory kinetics is subjected to decomposition temperatures, potential chain initiators form thermally at a very slow rate. Traces of the volatile product from this thermal degradation are observed but the fraction degraded in this manner is very small. Each chain initiator formed thermally is immediately destroyed by reaction with chain-terminating impurities present in the sample. After the impurity has reacted, it is no longer capable of acting as a chain terminator. The induction period represents a time during which thermally formed initiation sites react and remove chain-terminating impurities. Following the induction period there will be a brief period of overlap where some active sites will initiate chains and others will be destroyed by reaction with remaining impurities. When all impurities have been removed and each active site initiates a chain reaction, the ideal kinetics will then apply. For most samples studied in this work the period required for attaining ideal behavior probably does not exceed 10% degradation. During the acceleratory period the number of degrading chains increase. At the maximum rate the first started chains will go to completion. When a chain ceases degradation, it is removed from production. Beyond the maximum rate more chains are removed from production than are starting so the rate will decrease.

The mathematics that describes this non-steady-state behavior in terms of first-order initiation and zero-order chain degradation appears to be somewhat involved and complex even though it has been developed from very simple assumptions that are based on the zipper mechanism. Fortunately, the computer makes it simple to apply the mathematics of the NSSK model so that simplifying steady state assumptions are no longer necessary.

Acknowledgment

Acknowledgment is made to the donor of the Petroleum Research Fund administered by the ACS, for support of this work.

References

1. D. A. YOUNG, "Decomposition of Solids," Pergamon, London (1966).
2. P. W. M. JACOBS AND F. C. TOMPKINS, "Chemistry of the Solid State" (W. E. Garner, Ed.), Chap. 7, p. 184, Butterworths, London (1955).
3. P. G. FOX AND R. W. HUTCHINSON, *in* "Energetic Materials (H. D. Fair and R. F. Walker, Eds.), pp. 251–284, Plenum, New York (1977).
4. NG, WEE-LAM, *Aust. J. Chem.* **28**(6), 1169 (1975).
5. R. M. HAINES AND D. A. YOUNG, *Discuss. Faraday. Soc.* **31,** 229 (1961).
6. P. E. YANKWICH AND P. D. ZAVITSANOS, *J. Phys. Chem.* **68,** 457 (1964).
7. J. JACK, *J. Phys. Chem. Solids* **24,** 63 (1963).
8. B. V. EROFEEV, *C. R. Acad. Sci. USSR* **52,** 511 (1946).
9. M. J. AVRAMI, *J. Chem. Phys.* **7,** 1103 (1939); **8,** 212 (1940); **9,** 177 (1941).
10. J. D. DANFORTH AND T. TAKEUCHI, *J. Polym. Sci., Polym. Chem. Ed.* **11,** 2091 (1973).
11. J. D. DANFORTH, J. SPIEGEL, AND J. BLOOM, *J. Macromol. Sci.-Chem. A* **17,** 1107 (1982).
12. J. D. DANFORTH, *J. Macromol. Sci.-Chem.* **A19**(6), 897 (1983).
13. J. D. DANFORTH, U.S. Patent 3,431,477 (Mar. 4, 1969).

14. J. D. DANFORTH AND JAMES DIX, *J. Amer. Chem. Soc.* **93,** 6843 (1971).
15. J. D. DANFORTH, *in* "Computer Applications in Applied Polymer Science" (T. Provider, Ed.), ACS Symposium Series 197, pp. 377–384, Amer. Chem. Soc., Washington, D.C. (1982).
16. E. G. PROUT AND V. C. LIDDIARD, *J. Inorg. Nucl. Chem.* **35,** 2183 (1973).
17. R. W. HUTCHINSON, S. KLEINBERG, AND F. P. STEIN, *J. Phys. Chem.* **77,** 870 (1973).
18. BRUNO REITZNER, *J. Phys. Chem.* **65,** 948 (1961).
19. E. G. PROUT AND F. C. TOMPKINS, *Trans. Farad. Soc.* **40,** 488 (1944).
20. A. G. LEIGA, *J. Phys. Chem.* **70,** 3260 (1966).
21. J. Y. MACDONALD, *J. Chem. Soc.* 839 (1936).